# Experimental investigation of a compact ARC-based lead–graphite neutron activator for medical radionuclide production: the FESTA experiment

José A. Gálvez Altamirano*[1], Chalmin Ham[2], SangIn Bak[2], Chirag Kirtikumar Vyas[2], Kim DoYoon[2], Masoud Behzad[2], Seung-Woo Hong[2], Yacine Kadi[3], and Pierre Mandrillon[4]

[1]IBEL SA, Place du Molard 3, CH-1204 Geneva, Switzerland (affiliation at the time of the work)
[2]Department of Energy Science, Sungkyunkwan University, 2066 Seobu-Ro, Jangan-Gu, Suwon-Si, Gyeong Gi-Do, Republic of Korea
[3]CERN, Geneva, Switzerland (affiliation at the time of the work)
[4]AIMA Développement SA and MEDICYC, Centre Antoine Lacassagne, Nice, France (affiliations at the time of the work)

Experimental work documented in July 2015; synthesis prepared in 2026

**Abstract**

The Feasibility Study of the Activator (FESTA) investigated a compact accelerator-driven neutron activator based on the adiabatic resonance crossing (ARC) principle. Its primary technological motivation was the production of $^{99}$Mo, the parent radionuclide of $^{99m}$Tc, through neutron capture on $^{98}$Mo, with Lu, Re and Ho included as complementary medical-radionuclide targets. A 3.27 t lead diffuser surrounded by graphite, polyethylene and borated-polyethylene layers was constructed and tested at the MEDICYC cyclotron of the Centre Antoine Lacassagne in Nice. The campaign comprised 20 numbered run identifiers, with run 5 divided into two sub-runs, giving 21 tabulated irradiation entries. Irradiations used 60 MeV protons and approximately 29.4 MeV deuterons incident on a thick beryllium target at measured beam currents between 0.05 $\mu$A and 4.13 $\mu$A. Spatial activation was characterized using In, Au, W, Al, Zr, Sc and Cu monitors, together with natural or enriched Mo, Lu, Re and Ho targets. Activities were determined by calibrated high-purity germanium gamma spectrometry and compared with FLUKA and PHITS calculations. Across the proton cases tabulated in this synthesis, experiment-to-calculation ratios ranged from 0.45 to 3.20. For deuterons, the FLUKA calculations overpredicted many measured activities by factors of approximately 20–100, whereas PHITS reproduced the activity scale substantially better, with tabulated ratios from 0.52 to 3.12. The measurements provide evidence compatible with a spatially extended, broad resonance-relevant neutron field containing thermal, epithermal and fast-neutron activation components, although they do not independently establish its detailed energy spectrum. FESTA demonstrated experimental production of $^{99}$Mo, $^{177}$Lu, $^{188}$Re and $^{166}$Ho; production-scale operation, radiochemical separation, pharmaceutical-quality production and clinical dose delivery remained outside the demonstrated scope.

**Keywords:** accelerator-driven neutron source; $^{99}$Mo/$^{99m}$Tc; medical radionuclides; neutron activation; adiabatic resonance crossing; lead slowing-down; beryllium target; MEDICYC; FLUKA; PHITS.

## 1 Introduction

The primary technological motivation of FESTA was the local production of $^{99}$Mo, the parent radionuclide of $^{99m}$Tc, using an accelerator-driven neutron source. At the time of the experiment, the international supply of reactor-produced $^{99}$Mo was affected by the ageing of major research reactors and recurrent production interruptions. This situation motivated the investigation of alternative non-fission routes capable of supporting a more distributed supply of $^{99m}$Tc, the most widely used diagnostic radionuclide in nuclear medicine.

*Corresponding author. Email and present address to be inserted before submission.

The route investigated in FESTA was $^{98}$Mo(n,$\gamma$)$^{99}$Mo, followed by the beta decay of $^{99}$Mo and formation of $^{99m}$Tc. The long-term objective was therefore not direct irradiation production of $^{99m}$Tc, but production of its parent $^{99}$Mo, from which $^{99m}$Tc could subsequently be obtained through an appropriately designed generator and radiochemical process.

To enhance neutron capture in the resonance region, FESTA adopted the adiabatic resonance crossing (ARC) principle proposed by Carlo Rubbia and experimentally investigated in the TARC programme at CERN [2, 3]. In a high-purity lead medium, the high atomic mass of lead results in a small average logarithmic energy decrement per elastic collision, while its relatively low neutron-absorption probability permits neutrons to undergo many collisions. Their energy consequently decreases through small lethargy intervals, allowing the slowing-down population to traverse the resonance regions of capture target nuclides.

This behavior can produce a broad resonance-relevant neutron field and increase the probability that a neutron is captured while crossing a strong capture resonance. The FESTA activator combined a lead diffuser with graphite and polyethylene reflector–moderator regions to adapt this principle to a compact system driven by the MEDICYC cyclotron. Fast neutrons were generated by 60 MeV protons or approximately 29.4 MeV deuterons incident on a thick beryllium target. The physical rationale and the intended $^{99}$Mo/$^{99m}$Tc production chain are summarized in Figure 1.

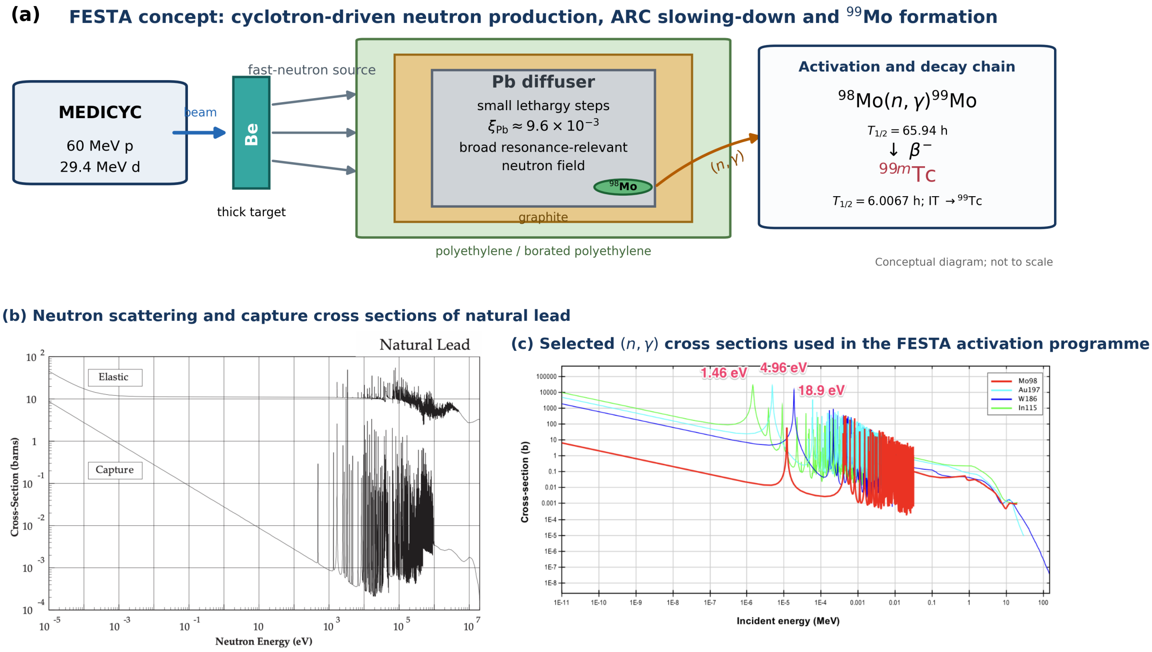


**Figure 1.** Physical rationale of the ARC-based FESTA activator. (a) Beam–target–activator and $^{98}$Mo(n,$\gamma$)$^{99}$Mo production chain. (b) Lead scattering and capture cross sections. (c) Capture cross sections of selected FESTA target nuclides. Panels (b) and (c) reproduce Figures 200 and 198 of the 2015 report.

FESTA must therefore be understood as an experimental investigation of whether the ARC principle could be transferred from the much larger, high-energy TARC configuration to a compact, medium-energy cyclotron-driven activator. Production of $^{99}$Mo was the principal medical objective, while activation of Lu, Re and Ho targets extended the investigation to other radionuclides of potential therapeutic interest.

The objectives of FESTA were to:

1. investigate production of $^{99}$Mo, as the parent radionuclide of $^{99m}$Tc, through the $^{98}$Mo(n,$\gamma$)$^{99}$Mo reaction;
2. construct and operate a compact cyclotron-driven neutron activator based on the ARC principle;
3. characterize spatial activation signatures associated with thermal, epithermal and fast-neutron components;
4. compare the measured activities with FLUKA and PHITS calculations;
5. investigate complementary activation routes leading to $^{177}$Lu, $^{188}$Re and $^{166}$Ho; and
6. identify the physical and engineering limitations relevant to subsequent optimization and scale-up.

This paper is a condensed scientific reconstruction of the 266-page FESTA final report prepared in July 2015 [1]. All numerical results are transcribed from that source unless explicitly identified as a new interpretation. No raw spectra, irradiation spreadsheets or Monte Carlo input decks were available for an independent re-analysis.

## 2 Project provenance and collaboration

FESTA was financed by IBEL SA and coordinated by José A. Gálvez on behalf of IBEL. The experimental work was conducted at the Centre Antoine Lacassagne (CAL) in Nice under the institutional and technical framework established with AIMA Développement SA and the management of CAL. The July 2015 report identifies IBEL SA, AIMA Développement SA, CAL and Sungkyunkwan University (SKKU) as members of the international collaboration [1].

The contemporaneous report identifies Dr Gálvez as its preparer under the contract between IBEL SA and Dr Gálvez. It states that the activator was developed within the CAL–AIMA–IBEL collaboration, constructed by IBEL, and assembled and tested at CAL. The project coordinator further records the scientific participation of Yacine Kadi of CERN and identifies Pierre Mandrillon as the AIMA and MEDICYC technical counterpart. The identified SKKU participants were Seung-Woo Hong, Chalmin Ham, SangIn Bak, Chirag Kirtikumar Vyas, Kim DoYoon and Masoud Behzad. Individual authorship for the present manuscript must be finalized only after each proposed author has reviewed and approved the text and accepted responsibility for the published work.

**Table 1.** Project bodies and contributions recorded for the FESTA programme. Institutional participation is distinct from individual authorship.

| Person or body | Role or affiliation | Recorded contribution |
|---|---|---|
| José A. Gálvez | IBEL SA | Project coordination, contractual representation of IBEL, responsibility for the experiment and preparation of the July 2015 final report. |
| IBEL SA | Geneva, Switzerland | Project financing; activator concept, engineering and construction; experimental programme. |
| Pierre Mandrillon | AIMA Développement SA | MEDICYC expertise, AIMA technical interface, and cyclotron and beam-line context. |
| AIMA Développement SA | France | Magnetic-field studies, MEDICYC settings, beam optics and definition of the irradiation-line elements. |
| Centre Antoine Lacassagne | Nice, France | Host laboratory, MEDICYC operation, facility agreement and experimental support. |
| Yacine Kadi | CERN | Scientific participation, as recorded by the project coordinator; detailed author contribution to be confirmed. |
| SKKU | Department of Energy Science, Sungkyunkwan University, Republic of Korea | Participating institution in the FESTA international collaboration; identified participants are listed below and individual CRediT contributions remain to be confirmed. |

The identified SKKU participants were Seung-Woo Hong, Chalmin Ham, SangIn Bak, Chirag Kirtikumar Vyas, Kim DoYoon and Masoud Behzad. Their institutional address was Department of Energy Science, Sungkyunkwan University, 2066 Seobu-Ro, Jangan-Gu, Suwon-Si, Gyeong Gi-Do, Republic of Korea.

## 3 Experimental facility and apparatus

### 3.1 MEDICYC beam and beryllium target

The experiment used the MEDICYC cyclotron at CAL. The documented irradiation energies were 60 MeV for protons and approximately 29.4 MeV for deuterons. A thick beryllium target, approximately 4 cm in diameter and 2 cm thick, converted the incident beam into a broad secondary-neutron source. The target assembly was water cooled and supported by thermal-hydraulic calculations. The target was optimized primarily for proton operation; its response to high-current deuterons was not experimentally qualified.

### 3.2 ARC-based compact activator

The activator contained approximately 3.27 t of high-purity lead in an assembly of about $0.6 \times 0.6 \times 0.8$ m. The lead constituted the principal slowing-down and neutron-diffusion medium required by the ARC concept.

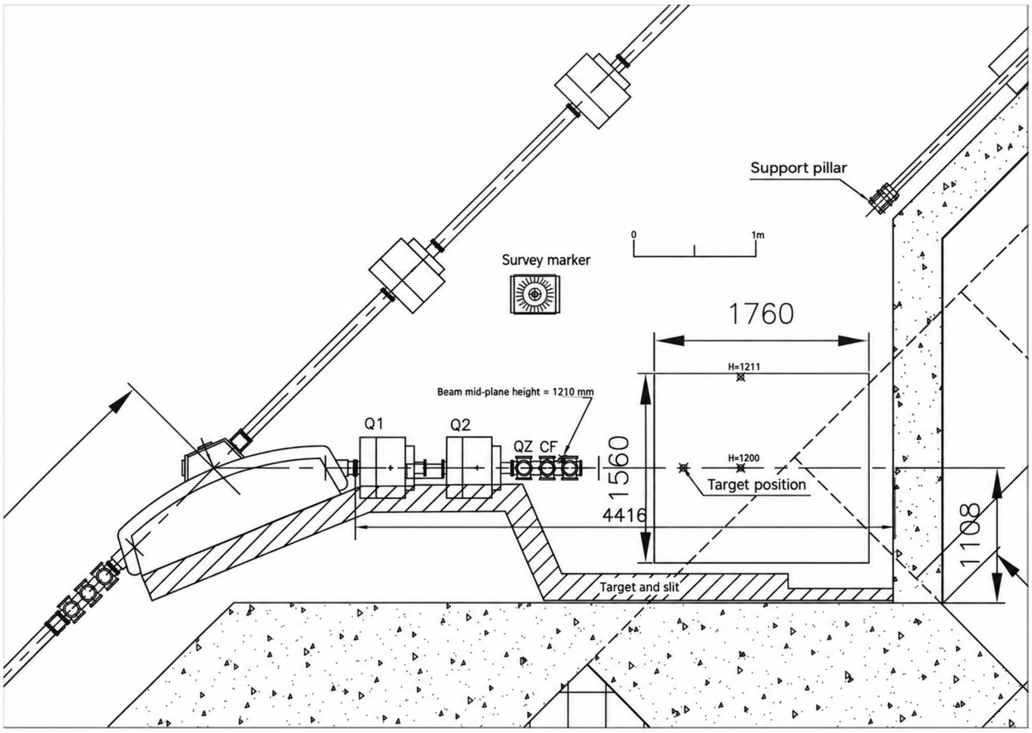


**Figure 2.** FESTA experimental configuration at the MEDICYC cyclotron. The extracted proton or deuteron beam impinged on the water-cooled beryllium target located at the lateral entrance of the activator. Secondary neutrons entered the lead-based assembly, while activation samples were inserted through tubes oriented perpendicular to the beam axis. The activator was supported on a base frame adjacent to the concrete shielding wall.

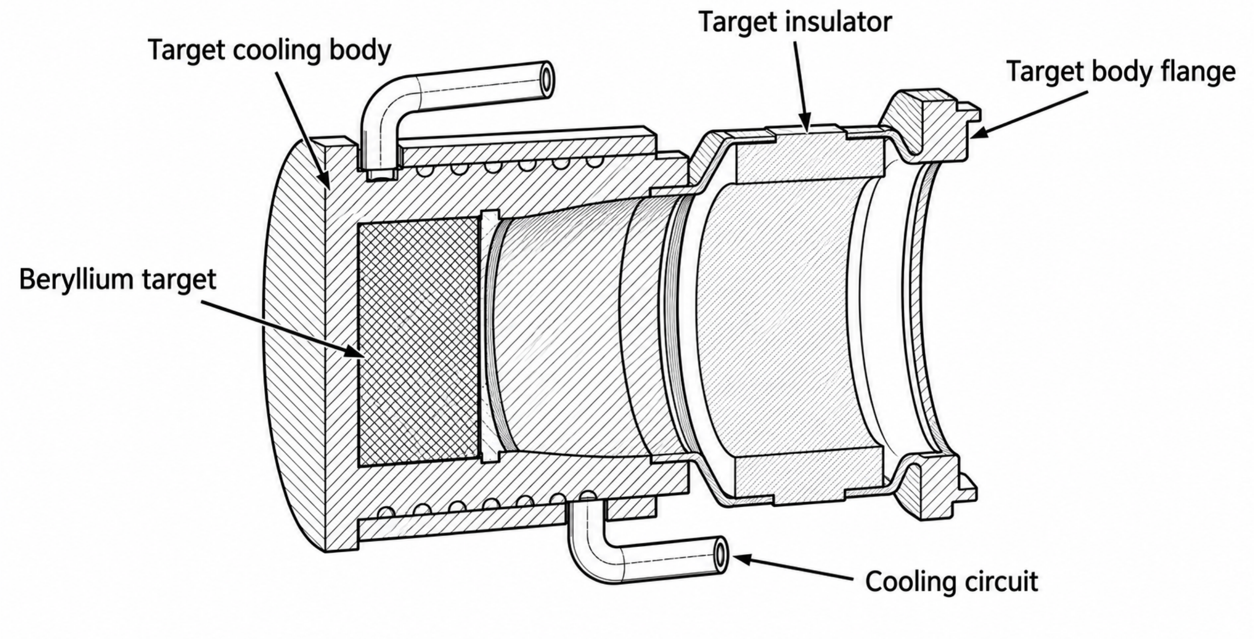


**Figure 3.** Thick beryllium neutron-production target and cooling assembly used in FESTA.

Graphite and polyethylene reflector–moderator layers increased neutron retention and modified the low-energy component, while polyethylene and borated-polyethylene provided external shielding. Ten access holes and several insertion depths provided up to 30 nominal sample positions distributed in layers A, B, −B and C. The beam axis and sample-insertion axes were orthogonal. The experimental configuration is summarized in Figures 2, 4 and 5.

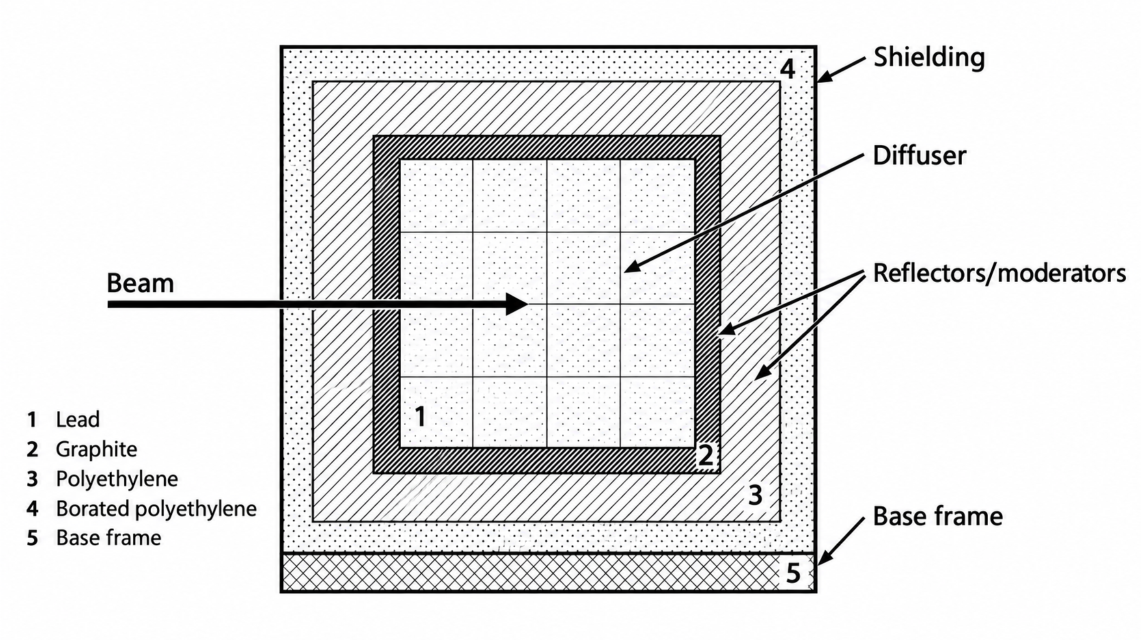


**Figure 4.** Layered geometry of the FESTA activator.

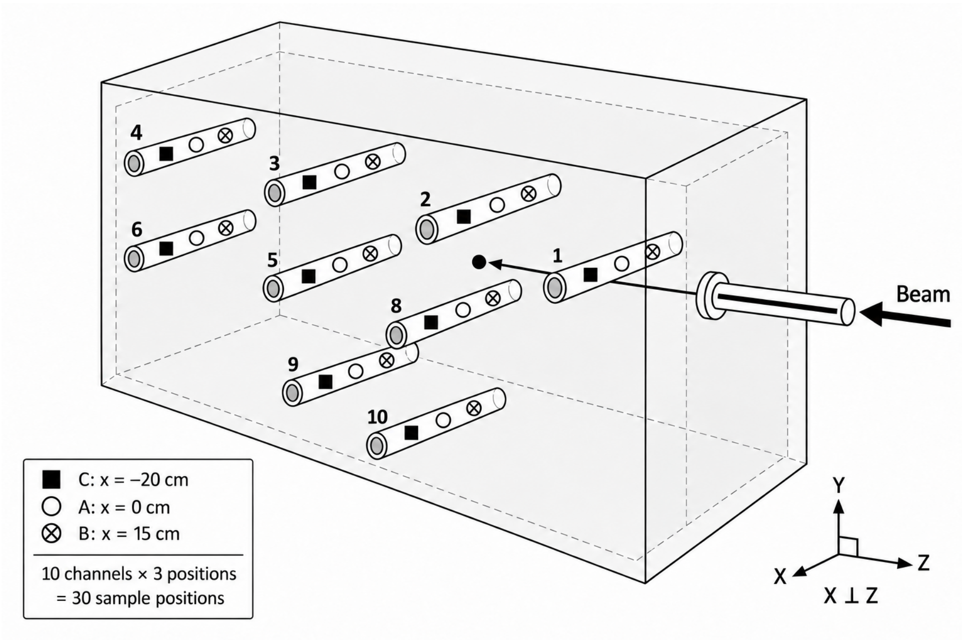


**Figure 5.** Sample layers, access holes and measurement positions inside the FESTA activator.

# 4 Irradiation programme

The report defines 20 run numbers; run 5 was executed twice (5a and 5b), giving 21 irradiation entries in Table 2. Proton or deuteron beams were used with average currents between 0.05 $\mu$A and 4.13 $\mu$A and irradiation times between 10 min and 60 min. The campaign varied sample material and position and included tests of layer symmetry, reflector/moderator changes, an open access hole and neutron leakage.

Activation monitors included natural In, Au and W for capture-dominated responses, Al and Zr for fast-neutron threshold reactions, and additional Sc and Cu samples. Medical-radionuclide target materials included natural and enriched Mo, natural Lu, natural Re and natural Ho. The principal product reactions considered in this synthesis are listed in Table 3.

**Table 2.** Beam conditions transcribed from Table 11 of the 2015 FESTA report.

| Run | Beam | Average current ($\mu$A) | Irradiation time (min) |
|---|---|---|---|
| 1 | p | 0.05 | 48.4 |
| 2 | p | 3.88 | 60 |
| 3 | p | 3.15 | 51 |
| 4 | p | 4.06 | 15 |
| 5a | p | 4.03 | 10 |
| 5b | p | 4.04 | 10 |
| 6 | p | 4.07 | 10 |
| 7 | p | 4.12 | 60 |
| 8 | p | 4.13 | 60 |
| 9 | p | 4.11 | 60 |
| 10 | d | 0.84 | 20 |
| 11 | p | 4.07 | 15 |
| 12 | d | 1.03 | 60 |
| 13 | p | 1.01 | 60 |
| 14 | p | 1.01 | 60 |
| 15 | p | 1.01 | 60 |
| 16 | p | 1.02 | 60 |
| 17 | p | 1.01 | 60 |
| 18 | d | 0.83 | 60 |
| 19 | d | 0.72 | 60 |
| 20 | p | 1.03 | 60 |

Run 5 was executed twice; entries 5a and 5b correspond to 05/Jan and 05/Feb, respectively, in Table 11 of the 2015 report.

**Table 3.** Principal activation routes relevant to the FESTA measurements.

| Target reaction | Product | Experimental purpose |
|---|---|---|
| $^{115}$In(n,$\gamma$)$^{116m}$In | $^{116m}$In | Thermal and resonance-sensitive activation monitor. |
| $^{197}$Au(n,$\gamma$)$^{198}$Au | $^{198}$Au | Reference capture monitor. |
| natW(n,$\gamma$)$^{187}$W | $^{187}$W | Epithermal-resonance response. |
| $^{27}$Al(n,$\alpha$)$^{24}$Na | $^{24}$Na | Fast-neutron threshold response. |
| $^{98}$Mo(n,$\gamma$)$^{99}$Mo | $^{99}$Mo | Parent radionuclide for $^{99m}$Tc; carrier-added route. |
| $^{176}$Lu(n,$\gamma$)$^{177}$Lu | $^{177}$Lu | Therapeutic radionuclide; carrier-added route. |
| $^{187}$Re(n,$\gamma$)$^{188}$Re | $^{188}$Re | Therapeutic radionuclide; carrier-added direct route. |
| $^{165}$Ho(n,$\gamma$)$^{166}$Ho | $^{166}$Ho | Therapeutic radionuclide and particulate-agent candidate. |

# 5 Gamma spectrometry and activity analysis

Irradiated samples were measured with a high-purity germanium detector and analysed using ORTEC GammaVision. Energy, peak-width and full-energy-peak efficiency calibrations were performed with multigamma standards over approximately 59–1800 keV. The calibration source and samples were measured in matching graphite-capsule geometry, thereby reducing a major geometry-dependent efficiency bias. Several spectra and gamma lines were used where possible, and final activities were obtained from weighted averages.

For a photopeak with net area $C_{\text{net}}$, the activity at the end of bombardment can be expressed as

$$A_{\text{EOB}} = \frac{\lambda C_{\text{net}}}{\varepsilon(E_\gamma) I_\gamma \exp(-\lambda t_{\text{cool}}) \left[1 - \exp(-\lambda t_{\text{real}})\right]} \frac{t_{\text{real}}}{t_{\text{live}}}, \tag{1}$$

where $\lambda$ is the decay constant, $\varepsilon(E_\gamma)$ is the full-energy-peak efficiency, $I_\gamma$ is the gamma-emission probability, $t_{\text{cool}}$ is the cooling time, and $t_{\text{real}}$ and $t_{\text{live}}$ are the real and live acquisition times. The exact implementation must be verified against the original GammaVision outputs if they become available.

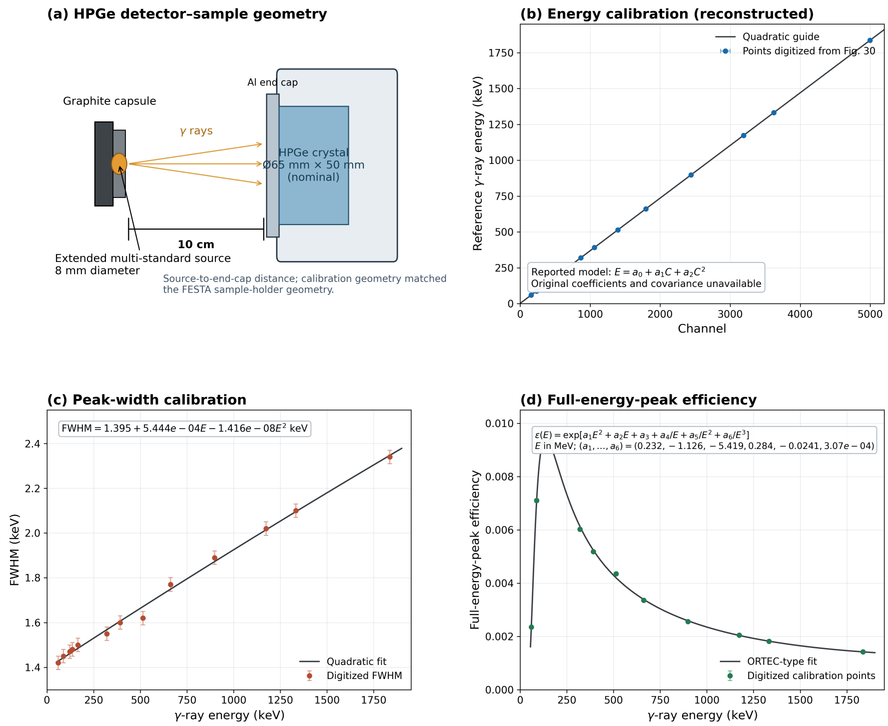


**Figure 6.** HPGe detector geometry and calibration information used in the FESTA activation analysis. (a) Detector–sample geometry, showing the graphite capsule, extended multigamma source, aluminium end cap and nominal HPGe crystal dimensions. (b) Reconstructed energy calibration from channel positions digitized from Figure 30 of the 2015 report. (c) FWHM calibration as a function of gamma-ray energy. (d) Full-energy-peak efficiency calibration with the reported ORTEC-type fit. Energy-channel and FWHM points were digitized from Figures 28–32; calibration residuals are not claimed. Efficiency error bars represent the certified source-activity uncertainties reported at approximately 95% confidence ($k = 2$).

## 5.1 Normalization to mass, current and irradiation time

For constant flux and a target population that is not significantly depleted, the EOB activity after an irradiation time $t$ is proportional to

$$1 - \exp(-\lambda t). \tag{2}$$

Therefore, conversion of a measured EOB activity $A(t)$ to the activity corresponding to a one-hour irradiation must use

$$A(1\,\text{h}) = A(t) \frac{1 - \exp[-\lambda(1\,\text{h})]}{1 - \exp(-\lambda t)}. \tag{3}$$

The complete normalization used to express the activity per target mass, average beam current and isotopic fraction at a reference irradiation time of one hour is

$$a_{1\mathrm{h}} = \frac{A_{\mathrm{EOB}}(t)}{mIf}\,\frac{1-\exp[-\lambda(1\,\mathrm{h})]}{1-\exp(-\lambda t)}. \tag{4}$$

Here $a_{1\mathrm{h}}$ denotes the activity normalized to a one-hour irradiation; the notation Bq/g/$\mu$A/h used in the report is retained as its reporting convention. The compact notation Bq/g/$\mu$A/h is used throughout this work to denote becquerels per gram per microampere per hour. Equation (3) gives only the time conversion, whereas Equation (4) also includes division by target mass $m$, average current $I$ and isotopic fraction $f$. The 2015 report states that the time normalization was checked by comparing measurements at equivalent sample positions after 10, 15 and 60 minutes of irradiation. The documentary limitations affecting independent recalculation are described in Section 10.

## 5.2 Uncertainty limitations

The report assigns global uncertainties of approximately 5–50%, depending on radionuclide, gamma line and counting statistics. At least one run carried a beam-current uncertainty of 22.5%. The surviving documentation does not provide a complete component-by-component covariance budget, and the raw spectra, calibration certificates and worksheets are unavailable. The recoverable uncertainty information is summarized in Table 4; unreported numerical components are not reconstructed retrospectively.

**Table 4.** Uncertainty information recoverable from the 2015 FESTA report.

| **Contribution** | **Quantitative information** | **Treatment in this synthesis** |
|---|---|---|
| Counting statistics and peak fitting | Included in reported global uncertainties; individual values not consistently recoverable | Values and error bars are reproduced from the report; no new fit was performed. |
| HPGe full-energy-peak efficiency | Calibration documented, but pointwise uncertainty and covariance unavailable | Not independently propagated. |
| Gamma-emission probability $I_\gamma$ | Nuclear-data values used in the original analysis; individual uncertainties unavailable | Not independently propagated. |
| Average beam current | One run explicitly reports 22.5%; a complete run-by-run budget is unavailable | Reported normalization retained without retrospective adjustment. |
| Target mass and isotopic fraction | Values documented for the targets; associated uncertainties not systematically reported | No additional numerical uncertainty assigned. |
| Self-absorption | Not corrected for some dense Lu, Re and W samples | Treated as a potential systematic bias. |
| Flux perturbation and resonance self-shielding | Not quantified | Relevant to scale-up; excluded from the reconstructed experimental uncertainty. |
| Combined uncertainty | Approximately 5–50%, depending on product and measurement | Reported range retained; correlations could not be reconstructed. |

# 6 Experimental results

## 6.1 Spatial activation and evidence of an extended neutron field

Capture products exhibited a broad spatial response across the activator, whereas threshold reactions decreased more rapidly with distance from the beryllium target. Comparable positions in layers B and −B were approximately symmetric. A lower-side deficit was associated with the iron support structure, indicating a non-negligible geometrical perturbation. Tests performed with an open access channel confirmed local neutron leakage, whereas the outer polyethylene and borated-polyethylene layers reduced external activation.

The activation measured at several irradiation positions provides experimental evidence that the lead–graphite assembly generated a spatially extended neutron field. The observation of capture and threshold-reaction products at locations distributed throughout the assembly is consistent with the presence of thermal, epithermal and fast-neutron components resulting from neutron production, moderation and transport beyond the immediate vicinity of the beryllium target.

These measurements do not, by themselves, constitute a complete validation of the energy-dependent neutron spectrum predicted for the ARC concept. Such validation would require multifoil spectral unfolding, including covariance treatment, or an independent neutron-spectrometry measurement together with a quantitative comparison against neutron-transport calculations. The experimental results should therefore be interpreted as evidence compatible with a broad, resonance-relevant neutron field.

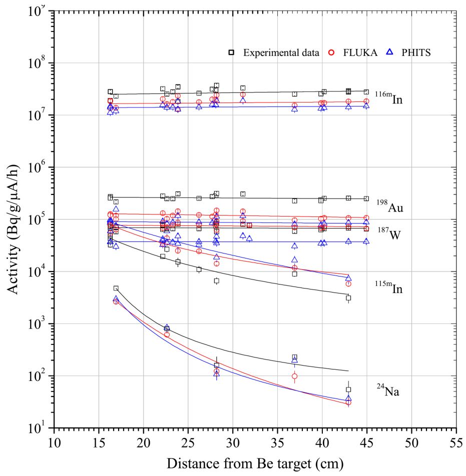


**(a)** 60 MeV protons.

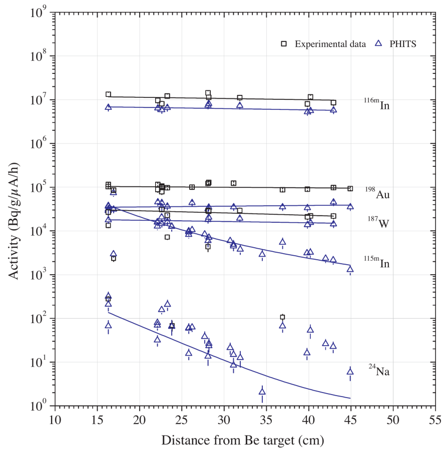


**(b)** 29.4 MeV deuterons.

**Figure 7.** Measured spatial activation profiles for selected capture and threshold products under (a) 60 MeV proton and (b) 29.4 MeV deuteron irradiation.

### 6.2 Medical-radionuclide targets

The principal medical target was enriched $^{98}$Mo, irradiated to produce $^{99}$Mo as the parent of $^{99m}$Tc. The programme also measured activation leading to $^{177}$Lu, $^{188}$Re and $^{166}$Ho. Table 5 lists the best-position specific activities quoted in the final report for proton irradiation. These values are useful for comparing target responses within the experiment; their time-normalization consistency was verified as described in Section 5.1, although they were not independently recalculated from the original gamma spectra.

**Table 5.** Best-position specific activities reported in the 2015 FESTA report for 60 MeV proton irradiation.

| Activation route | Product | Reported activity[a] | Interpretation |
|---|---|---|---|
| $^{98}$Mo(n,$\gamma$) | $^{99}$Mo | 7.59*e*3 Bq/g/$\mu$A/h | Measured enriched-Mo route. |
| natLu(n,$\gamma$) | $^{177}$Lu | 4.27*e*4 Bq/g/$\mu$A/h | Measured with natural Lu. |
| $^{176}$Lu(n,$\gamma$) | $^{177}$Lu | 1.65*e*6 Bq/g/$\mu$A/h | Enrichment-scaled value; not a separate full-scale target test. |
| $^{187}$Re(n,$\gamma$) | $^{188}$Re | 1.41*e*5 Bq/g/$\mu$A/h | Measured natural-Re route. |
| $^{165}$Ho(n,$\gamma$) | $^{166}$Ho | 4.76*e*5 Bq/g/$\mu$A/h | Measured natural-Ho route. |

[a] Units are Bq/g/$\mu$A/h. Values transcribed from the best-location row of Table 73 in the 2015 report and not independently

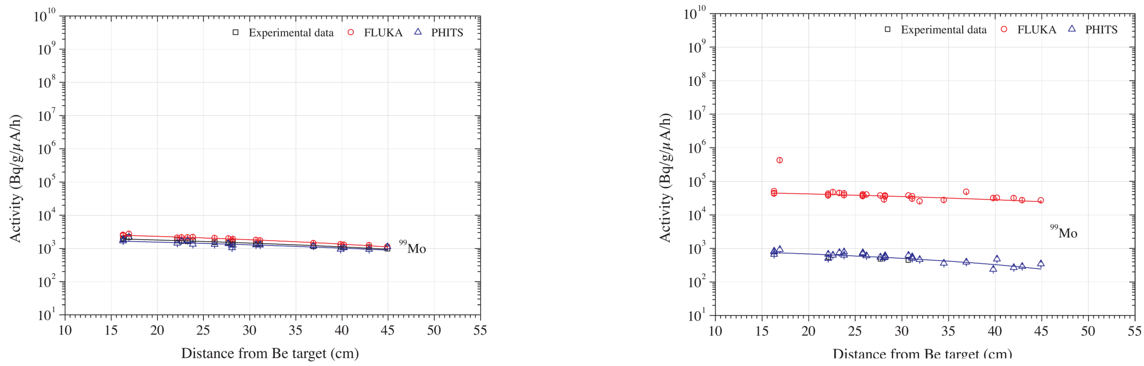


**(a)** Proton irradiation.

**(b)** Deuteron irradiation.

**Figure 8.** Spatial activity profiles for the medical-radionuclide target materials.

## 7 Monte Carlo benchmark

The simulations modelled the beryllium target, lead diffuser, reflector/moderator layers, shielding and sample positions. FLUKA [4] and PHITS [5] were compared with measured activities. The calculation tests two coupled problems: production of secondary neutrons by protons or deuterons on thick beryllium, and transport of the resulting field through the activation geometry.

### 7.1 Activation monitors

The average experimental-to-calculated ratios reported for representative activation products are summarized in Table 6. For protons, the ratios span approximately 0.45–2.94 across the listed reactions and codes. For deuterons, FLUKA overpredicts the activity severely: Data/MC values of 0.01–0.04 correspond to calculation-to-data discrepancies of factors 25–100. PHITS gives a much closer activity scale, although reaction-dependent deviations remain.

**Table 6.** Average experiment-to-calculation activity ratios for selected activation monitors.

| Beam | Product | Exp/FLUKA (dimensionless) | Exp/PHITS (dimensionless) |
|---|---|---|---|
| p | $^{116m}$In | 1.52 | 1.90 |
| p | $^{115m}$In | 0.58 | 0.45 |
| p | $^{198}$Au | 2.24 | 2.94 |
| p | $^{187}$W | 0.92 | 1.85 |
| p | $^{24}$Na | 1.71 | 1.35 |
| p | $^{97}$Zr | 1.29 | 1.48 |
| d | $^{116m}$In | 0.03 | 1.67 |
| d | $^{115m}$In | 0.02 | 0.52 |
| d | $^{198}$Au | 0.04 | 2.80 |
| d | $^{187}$W | 0.02 | 1.56 |
| d | $^{24}$Na | 0.01 | 1.19 |

## 7.2 Medical-radionuclide targets

The medical-target comparisons in Table 7 show the same qualitative behavior. Under proton irradiation, the activity scale is reproduced within route-dependent factors of approximately 0.8–3.2. Under deuteron irradiation, the FLUKA discrepancy persists at factors of approximately 20–100, whereas PHITS produces ratios between 0.89 and 3.12 for the listed cases.

**Table 7.** Average experiment-to-calculation activity ratios for the medical-radionuclide targets.

| Beam | Route | Exp/FLUKA (dimensionless) | Exp/PHITS (dimensionless) |
|---|---|---|---|
| p | natMo → $^{99}$Mo | 0.80 | 1.11 |
| p | $^{98}$Mo → $^{99}$Mo | 0.82 | 1.53 |
| p | natRe → $^{188}$Re | 1.16 | 1.72 |
| p | natLu → $^{177}$Lu | 2.59 | 3.20 |
| p | natHo → $^{166}$Ho | — | 3.03 |
| d | natMo → $^{99}$Mo | 0.01 | 0.89 |
| d | $^{98}$Mo → $^{99}$Mo | 0.02 | 1.59 |
| d | natRe → $^{188}$Re | 0.02 | 1.75 |
| d | natLu → $^{177}$Lu | 0.05 | 3.12 |
| d | natHo → $^{166}$Ho | — | 2.91 |

The consistent deuteron discrepancy across several reactions is unlikely to arise solely from a single gamma line, detector-efficiency value or target sample. It is consistent with a deficiency in the deuteron-on-beryllium neutron-source description used in the original FLUKA calculation.

The 2015 FESTA report states that deuterons were transported using the `SDUM = IONSPLIT` option and that this treatment did not reproduce the deuteron-breakup process correctly. This limitation is physically important because breakup neutrons exhibit a correlated angular–energy distribution that determines both their forward yield and their subsequent transport through the activator. Independent thick-target measurements likewise show the strong energy- and angle-dependent character of neutron production from deuterons on beryllium [6].

The absence of the original FLUKA input decks prevents a more detailed reconstruction of the model settings; consequently, the observed discrepancy should be regarded as a benchmark of the calculation used in 2015, rather than as a general assessment of current FLUKA capabilities.

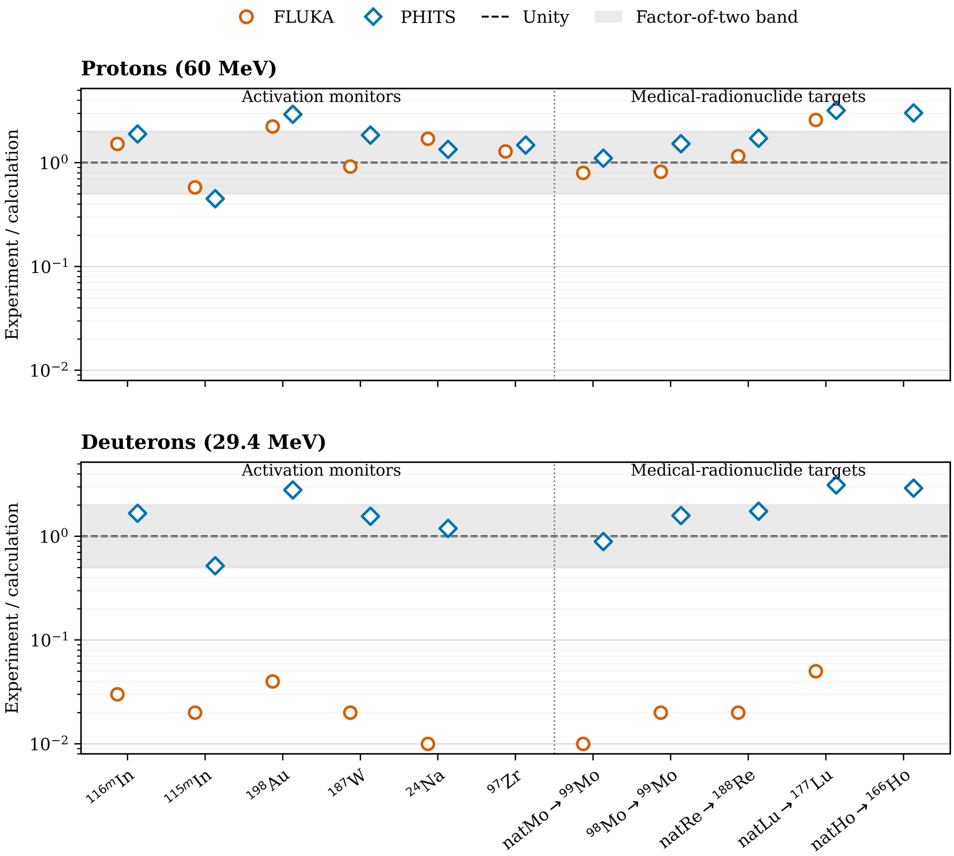


**Figure 9.** Experiment-to-calculation activity ratios for proton and deuteron irradiations. The dashed line denotes unity and the shaded region agreement within a factor of two.

# 8 Interpretation for medical radionuclides

The FESTA activities demonstrate nuclear production, not a finished radiopharmaceutical. Translation to medical use requires radionuclidic and radiochemical purity, activity per mole, stable-carrier quantification, target recovery, chemical processing yield, validated formulation, sterility, endotoxin control and dosimetry.

For $^{99}$Mo, the $^{98}$Mo(n,$\gamma$) route is carrier added and yields low-specific-activity $^{99}$Mo compared with fission production. A clinically meaningful $^{99}$Mo/$^{99m}$Tc assessment must include Bateman ingrowth, branching, generator loading, elution efficiency, elution schedule and processing losses. It is not physically correct to equate measured $^{99}$Mo activity directly with an injected $^{99m}$Tc patient dose.

The measured $^{99}$Mo activity can nevertheless be used as the initial condition for a Bateman ingrowth calculation and thereby to estimate an idealized upper bound on the $^{99m}$Tc activity available at a specified generator-elution time. Such an upper bound would assume 100% recovery and generator loading, no processing or transport losses, complete retention of the parent nuclide and ideal elution efficiency; it must still include the physical decay of $^{99}$Mo and the simultaneous ingrowth and decay of $^{99m}$Tc.

For $^{177}$Lu, direct neutron capture on $^{176}$Lu also produces a carrier-added product. The intended radiopharmaceutical determines whether the attainable molar activity is sufficient, and the long-lived $^{177m}$Lu impurity must be evaluated. This route must be distinguished from indirect no-carrier-added production schemes.

Direct capture production of $^{188}$Re is likewise carrier added, while clinical supply is often associated with a $^{188}$W/$^{188}$Re generator. $^{166}$Ho may be better suited to particulate or macroscopic carrier applications, but its formulation, activity per mass and dosimetry remain application specific.

# 9 Engineering and scale-up limitations

FESTA demonstrated mechanical assembly, low-current proton and deuteron irradiation, a water-cooled target concept, sample handling and neutron-shielding behavior. It did not demonstrate sustained operation at the currents required for production. A production design would require:

- continuous high-current operation with thermal transients and beam-trip analysis;
- beryllium-target lifetime, blistering, corrosion, water activation, leak detection and remote replacement;
- remote target insertion and retrieval, hot-cell transfer and occupational-dose optimization;
- structural activation, maintenance access, waste classification and decommissioning analysis;
- removal or redesign of the iron support that perturbed the lower neutron field;
- a geometry optimized for production rather than flexible experimental access; and
- validated radiochemical processing and GMP-compatible material flow.

The scaling presented in Table 8 reconstructs the prospective calculation contained in the contemporaneous conversion worksheet, in which 65 $\mu$A was the upper proton-current objective envisaged for a possible future MEDICYC/CAL upgrade rather than an experimentally attained current. It should not be interpreted as a validated production prediction. Strict linear extrapolation to a 100 g target, a 65 $\mu$A beam current and a 10 h irradiation does not account for resonance self-shielding, neutron-flux depression, activity saturation, target-geometry effects or heat-removal limitations. Furthermore, dividing the projected $^{99}$Mo activity by 555 MBq does not directly determine the number of injectable $^{99m}$Tc patient doses. Such an estimate would require modelling of $^{99}$Mo/$^{99m}$Tc ingrowth, decay and branching, radiochemical recovery, generator loading, elution efficiency and schedule, processing and transport losses, radionuclidic purity, and the administered-activity protocol.

# 10 Data and document availability

The primary source used for this synthesis is the 266-page file `Report Final and Annex 123.pdf`, with PDF creation metadata dated 21 July 2015. Its SHA-256 fingerprint is:

```
f92a3d526991469b1547d2df8dedff45c0caeb5a9d4dad359fb698ea479b7c68
```

This fingerprint identifies the exact document from which the numerical tables and historical statements were extracted. The original report should remain unchanged. Any corrections should be published in this synthesis or in a separate erratum with an explicit revision history.

**Table 8.** Measured specific activities and prospective production estimates reconstructed from Table 73 of the 2015 FESTA final report.

| **Quantity** | $^{99}$**Mo** | $^{177}$**Lu** (nat.) | $^{177}$**Lu** (enr.) | $^{188}$**Re** | $^{166}$**Ho** |
|---|---|---|---|---|---|
| Measured specific activity (best location) (Bq/g/$\mu$A/h) | $7.59 \times 10^3$ | $4.27 \times 10^4$ | $1.65 \times 10^6$ | $1.41 \times 10^5$ | $4.76 \times 10^5$ |
| Specific activity (MBq/g/$\mu$A/h) | $7.59 \times 10^{-3}$ | $4.27 \times 10^{-2}$ | 1.65 | $1.41 \times 10^{-1}$ | $4.76 \times 10^{-1}$ |
| *Prospective MEDICYC/CAL upgrade scenario* | | | | | |
| Assumed current ($\mu$A) | 65 | 65 | 65 | 65 | 65 |
| Assumed target mass (g) | 100 | 100 | 100 | 100 | 100 |
| Assumed irradiation time (h) | 10 | 10 | 10 | 10 | 10 |
| Linearly projected activity (GBq) | 0.49 | 2.78 | 107 | 9.17 | 30.9 |
| Reference activity used in the original table (MBq) | 555 | 5550 | 5550 | 5550 | 5550 |
| Projected activity/reference-activity ratio | 0.89 | 0.50 | 19.31 | 1.65 | 5.57 |

The specific activities are reported experimental values at the best irradiation location. They have not been independently recalculated from the original gamma spectra.
The assumed 65 $\mu$A current represents a prospective MEDICYC/CAL upgrade condition. This value was the upper proton-current objective envisaged in the 2015 report for a possible future upgrade, rather than a current attained during the experiment. The maximum average current documented during the FESTA irradiations was 4.13 $\mu$A.
Projected activities were calculated by linear scaling to a 100 g target and a 10 h irradiation. These projections do not include saturation, resonance self-shielding, neutron-flux depression, target heating or processing losses.
The activity/reference-activity ratios reproduce the arithmetic procedure used in Table 73. They are not demonstrated numbers of clinically deliverable patient doses.
The final two rows of the original Table 73, entitled "Amplification factor needed to produce 1 Ci/day" and "Number of Daily Doses", are not reproduced because their derivation cannot be reconstructed from the preceding rows without introducing additional undocumented assumptions.
The values in the row "Linearly projected activity" reproduce the arithmetic used in the contemporaneous conversion worksheet:

$$A_{\mathrm{proj,lin}} = a_{1\mathrm{h}}\, m_{\mathrm{assumed}}\, I_{\mathrm{assumed}}\, t_{\mathrm{assumed}}.$$

For $^{99}$Mo,

$$A_{\mathrm{proj,lin}} = (7.59 \times 10^{-3})(100)(65)(10) = 493\,\mathrm{MBq} \simeq 0.49\,\mathrm{GBq}.$$

This expression is reported solely to document the original projection. Because radioactive build-up is not linear with irradiation time, a physically corrected projection to an irradiation time $T$ would instead require the factor

$$\frac{1 - \exp(-\lambda T)}{1 - \exp[-\lambda(1\,\mathrm{h})]},$$

together with corrections for self-shielding, flux depression and target geometry.

The raw gamma spectra, calibration certificates, run spreadsheets and Monte Carlo input decks were not available during preparation of this manuscript. Their absence prevents an independent numerical re-analysis but does not negate the existence or historical value of the documented experimental campaign.

# 11 Conclusions

FESTA realized and operated a compact accelerator-driven neutron activator based on the ARC principle and produced an extensive spatial activation data set with proton and deuteron beams. Its principal technological objective was to investigate production of $^{99}$Mo, as the parent radionuclide of $^{99m}$Tc, through neutron capture on $^{98}$Mo. The experiment demonstrated production of $^{99}$Mo in the FESTA geometry and extended the measurements to $^{177}$Lu, $^{188}$Re and $^{166}$Ho.

The spatial activation measurements provide evidence compatible with a broad resonance-relevant neutron field containing thermal, epithermal and fast-neutron components. They do not, in the absence of spectral unfolding or independent neutron spectrometry, constitute a complete validation of a unique ARC neutron spectrum.

Although $^{99}$Mo production was the principal technological motivation of FESTA, one of the strongest quantitative results preserved in the experimental record is the benchmark of neutron production and transport calculations. Proton-induced activation was reproduced at an order-of-unity level with reaction-dependent bias.

For the deuteron irradiations, the tabulated experiment-to-FLUKA ratios were approximately 0.01–0.05, corresponding to calculation-to-data factors of approximately 20–100, while PHITS was substantially closer. This provides a valuable benchmark for deuteron-on-beryllium neutron-source modelling coupled to transport in a lead-based activator.

The experiment did not establish sustained high-current operation, industrial competitiveness, pharmaceutical-quality production or clinical dose delivery. These are separate development stages. Publication of the existing benchmark does not require repetition of the original campaign. New irradiations would be justified only to support new claims, such as high-current performance, a revised geometry, modern transport-code validation or a complete radiochemical production chain.


# Acknowledgements

The authors acknowledge IBEL SA for financing and supporting the FESTA experimental programme. In particular, they recognize the contributions of Igor Malishkov and Rafael Gimalov as investors, Kirill Tulskiy for project management, and Sergei Kulish as a member of the IBEL SA team.

The experiment was coordinated by José A. Gálvez on behalf of IBEL SA and carried out at the Centre Antoine Lacassagne in Nice in cooperation with AIMA Développement SA, and the scientific collaborators identified in this article from CERN and Sungkyunkwan University in the FESTA programme. They also acknowledge the technical and operational personnel of MEDICYC and CAL who supported preparation and execution of the irradiation campaign.


# Author contributions

**José A. Gálvez Altamirano:** Conceptualization; Methodology; Project administration; Investigation; Supervision; Formal analysis; Writing – original draft; Writing – review and editing.

**Chalmin Ham, SangIn Bak, Chirag Kirtikumar Vyas, Kim DoYoon and Masoud Behzad:** Investigation; Data curation; Formal analysis. The individual allocation of these activities is to be confirmed by the contributors before submission.

**Seung-Woo Hong:** Investigation; Supervision of the SKKU experimental group; Formal analysis; Validation; Writing – review and editing.

**Yacine Kadi:** Conceptualization; Methodology; Supervision; Validation; Formal analysis; Writing – review and editing.

**Pierre Mandrillon:** Methodology; Resources; Investigation; Supervision; Writing – review and editing.

## Funding

The FESTA experimental programme was financed by IBEL SA, with investment support from Igor Malishkov and Rafael Gimalov.

## Competing interests

José A. Gálvez Altamirano represented IBEL SA during the FESTA programme. Any intellectual-property interests, contractual rights or subsequent commercial relationships relevant to the activator should be declared before submission.

## References

[1] J. A. Gálvez, *Feasibility Study of the Activator (FESTA): Final Report and Annexes*, IBEL SA, Geneva, July 2015, 266 pp.

[2] C. Rubbia, *Resonance Enhanced Neutron Captures for Element Activation and Waste Transmutation*, CERN-LHC/97-04-EET, CERN, Geneva, 1997.

[3] A. Abánades et al., Results from the TARC experiment: spallation neutron phenomenology in lead and neutron-driven nuclear transmutation by adiabatic resonance crossing, *Nucl. Instrum. Methods Phys. Res. A* **478** (2002) 577–730.

[4] A. Ferrari, P. R. Sala, A. Fassò and J. Ranft, *FLUKA: A Multi-Particle Transport Code*, CERN-2005-010, INFN/TC_05/11, SLAC-R-773, 2005.

[5] T. Sato et al., Particle and Heavy Ion Transport code System, PHITS, version 2.52, *J. Nucl. Sci. Technol.* **50** (2013) 913–923, doi:10.1080/00223131.2013.814553.

[6] T. Aoki et al., Measurements of differential thick-target neutron yields and $^{7}$Be production in Li and $^{9}$Be(d,n) reactions for 25 MeV deuterons, *J. Nucl. Sci. Technol.* **41** (2004) 399–405, doi:10.1080/18811248.2004.9715501.